

**VSP case study
of an apparent seismic anomaly
along the crest of a Leduc reef**

Ronald C. Hinds*

and

Neil L. Anderson+

* Dept. of Geology, University of Pretoria, Pretoria, South Africa, 0002

+ Kansas Geological Survey, University of Kansas, Lawrence, Kansas 66047

Abstract

On the basis of conventional surface seismic data, an exploratory well (referred to as the VSP well) was drilled into the updip, raised rim of the Leduc Formation (Devonian Woodbend Group) reef complex at Lanaway Field, southeastern Alberta, Canada. The well was expected to encounter an anomalous late-stage accretionary buildup at the Leduc level. It was anticipated that the Leduc at the VSP well location would be up to 80 m higher than at adjacent rim well sites. To the consternation of the geophysicists, the envisioned accretionary growth was not present; the top of the Leduc in the VSP well was consistent with other rim wells and inconsistent with the seismic interpretation. Fortunately, however, the Leduc was structurally closed and the VSP well was completed as an oil producer (from both the Nisku and Leduc formations).

In order to resolve the apparent discrepancy between the interpreted surface seismic data and geology at the VSP well, a vertical seismic profile (VSP) was conducted at the well site. The interpretation of the VSP data was expected to elucidate the geological origin of the misinterpreted seismic anomaly. Towards this end, the VSP was relatively successful. These data confirmed that the original interpretation of the surface seismic data (with respect to the Nisku, Ireton and Leduc top) was incorrect, and that the anomaly observed on the surface seismic line was not a processing artifact. It was ultimately attributed to several superposed effects: 1) anomalous structural relief at the pre-Cretaceous subcrop; 2) stratigraphic anomalies within the Winterburn Group; 3) multiple interference; and 4) tuning effects associated with the thinning of the Ireton along the seismic profile.

Introduction

The Woodbend Group in central Alberta (Figure 1) is subdivided into four formations: Cooking Lake, Duvernay, Leduc, and Ireton. The Cooking Lake is platform facies. The Leduc is reefal facies; the Duvernay and Ireton are inter-reef shales (Anderson et al., 1989a, b; Klován, 1964; McNamara and Wardlaw, 1991; Moore, 1988, 1989a, 1989b; Mossop, 1972; Mountjoy, 1980; Stoakes, 1980; and Stoakes and Wendte, 1987).

The Leduc Formation at Lanaway (Figures 2 and 3) is classified as a large atoll. It towers some 200 m above the Cooking Lake platform and exhibits a mappable raised (peripheral) rim and a structurally lower central lagoonal area. Such raised rims are described in Mossop (1972) in his study of the isolated Leduc Formation limestone reef complex at Redwater. In that study the raised rim was postulated to arise primarily as a result of the differential compaction of rigid reef facies and central lagoonal facies. The updip edge (to the northeast) of the raised rim at Lanaway is productive where the reef is structurally closed and effectively sealed by the inter-reef shales of the Duvernay and Ireton Formations. Geologic cross-sections shown in Figures 4, 5 and 6 (well locations shown in Figure 3) illustrate the interpreted morphological relationships between the Leduc and inter-reef shales of the Ireton and Duvernay in the Lanaway area.

On seismic data, Lanaway Leduc reef is readily differentiated from inter-reef shales. The carbonate buildup is characterized by appreciable velocity pullup (25 ms), time-structural drape at the top of the Devonian (25 ms) and character variations within the Woodbend Group (associated with the abrupt transition from shale to reefal facies). Back from the steeply dipping edge, the top of the reef is clearly defined on seismic data, being manifested as a high-amplitude peak on

normal polarity data.

In this paper, we discuss the 2-D seismic and VSP signatures of the top of the Leduc reef at Lanaway. The 2-D data were acquired prior to drilling the VSP well, which ultimately ended up intersecting the reef some 80 m below prognosis. The VSP survey was run in an attempt to resolve the apparent discrepancy between the interpreted surface seismic data and the geology at the exploratory (VSP) well.

Lanaway Field

Full Leduc reef at Lanaway Field towers up to 200 m above the Cooking Lake platform and exhibits a raised rim (Figures 4 and 5) and a structurally low interior lagoon. Leduc production is restricted to the updip eastern edge of the reef complex (up to 50 m of pay). The eastern and western limits of production are defined by the fore-reef slope and the hydrocarbon/water interface, respectively.

The structural geologic cross-sections of Figures 4, 5 and 6 illustrate the morphology of the Lanaway complex. Well 10-29 (Figure 4) is off-reef and encountered a full section of inter-reef shale (Ireton and Duvernay); 11-1 is interpreted as having penetrated the structurally low and wet interior lagoon; 16-1 and 11-6 were drilled into the updip raised rim of the Lanaway complex and are productive. 11-36 (Figure 5) is interpreted as having penetrated the structurally low and wet interior lagoon; 2-36 and the VSP well were drilled into the raised rim of the Lanaway complex. The VSP well is productive. Well 2-36 penetrated the Leduc below the hydrocarbon/water contact, however it is classified as a Nisku oil well with extended productivity from the Viking (gas) and Basal Quartz (oil). The VSP well has a different oil/water contact than 11-6 to the north and, consequently,

is assigned to a separate pool. The hydrological barrier between these two wells is related to structural relief at the Leduc level (Figure 6). This relief could be due to several processes or features including surge channels, shale tongues, differential compaction, or original reef morphology (Anderson, 1989a and b; Klovan, 1964; Mossop, 1972).

The VSP well (Figures 5 and 6), although ultimately productive (from both the Nisku and Leduc) was 80 m low at the Leduc level relative to the original seismic prognosis. This pre-drill structural estimate was based on the conventional seismic data interpretation displayed as Figures 7 and 8. In this original interpretation, the Leduc event is up to 30 ms (80 m) higher between CDP traces 100 and 140 than elsewhere. Geologically, this anomaly was initially envisioned as localized, late stage accretionary reef growth. The drilling of the VSP well however, established that on the original interpretation, the top of the Leduc was miscorrelated by one cycle (between CDP traces 100 and 140). Well log data established that at the VSP well, the Leduc top was more-or-less time-structurally consistent with the top of the Leduc elsewhere on the seismic line.

VSP acquisition

In an effort to resolve the apparent discrepancy between the surface seismic data (as originally interpreted; Figures 7 and 8) and the Leduc top at the VSP well, a VSP survey was conducted at that well site. The interpretation of the VSP was expected to elucidate:

- 1) The geological significance (if any) of the misinterpreted seismic anomaly;
and

- 2) The effect of possible multiple interference on the seismic data.

The VSP data were acquired at a single surface offset, located 200 m to the west of the VSP well on the lease access road. The source consisted of two in-series Vibroseis units utilizing an 8 to 96 Hz input sweep (designed to be compatible with the frequency content of the existing surface seismic data). The Vibroseis sweep was 13 seconds in duration and the recording length was 19 seconds, resulting in a 3 s long cross-correlated output time series. On average, six sweeps were summed for each subsurface geophone sonde location. The source site was partially frozen and suitable coupling was achieved. The Vibroseis pad location at the offset was shifted periodically by a minor amount to ensure ground coupling stability and minimize damage to the surface of the lease access road.

TD (total depth) of the VSP well was 2990 m below KB (Kelly Bushing) at the time of the running of the VSP survey. The elevation of the KB was 968 m asl (above sea level); the source was 963 m asl. The geophone sonde was lowered to TD, then raised at 20 m intervals to 2590 m (30 m above the Wabamun Formation; Figure 1). Between 2590 and 1315 m (shallowest processed sonde depth location), the sonde interval was increased to 25 m. Only three levels were collected above 1315 (at 600, 1000 and 1150 m). These data were acquired principally for sonigram calibration purposes. At each sonde location, the three component geophone tool was locked in place in the borehole with the locking arm.

The data were recorded at a 2 ms sample interval recording instruments using the SSC 1078 micro-Vax based system. The recording filter was OUT/OUT.

The offset location was situated behind a bend in the road so that the source was not in direct line of sight of the well borehole. A patch of trees was in the

corner of the road between the source and the well. This aided in the elimination of groundroll induced interference (tube waves) with the downgoing and upgoing signal.

VSP interpretive processing

As an aid to the interpretation of the VSP data a suite of interpretive processing panels (IPP's) were generated for these data. The panels allow for the progressive interpretation of the data and facilitate the quality control of the processing sequence. More specifically the panels display:

- 1) Up and downgoing P-wavefield separation;
- 2) Deconvolution of the separated upgoing P-waves using the inverse filter calculated from the separated downgoing P waves; and
- 3) Inside and outside corridor stacks of both the deconvolved and non-deconvolved upgoing P-waves.

Throughout the paper, the abbreviations FRT, -TT time and +TT time are used repeatedly. FRT is the abbreviation for field recorded time, the term used to describe the time-depth display of the raw field records. The terms -TT and +TT refer to specific data configurations. Specifically, -TT is used in reference to the data display on which the first breaks and downgoing waves are aligned and bulk shifted. On these displays the first break traveltimes for each trace has been subtracted from that trace, and the aligned traces have been bulk-shifted to an arbitrary time-datum (usually to 100 or 200 ms). The term +TT is used in reference to the data display on which the first break time of each trace has been

added to that trace (plus possible normal moveout correction for the non-zero offset source). On the +TT displays the upgoing waves the upgoing waves are aligned.

P-wave separation

In the initial phase of processing, the upgoing and downgoing P-waves of the vertical (Z) geophone data were separated. This separation procedure is illustrated in the wavefield separation IPP in Figure 9.

In panels 1 and 2 (Figure 9), the field Z data after trace normalization and the gained Z data are displayed, respectively. Several primary upgoing reflection can be identified on these data: Viking (at a depth of 2100 m); Mannville (the Glauconitic at 2158 m); and Banff (2293 m). Note that the series of strong reflections that originate below the VSP well TD do not intersect the first break curve, and therefore cannot be confidently classified as either primary or multiple events.

The gained VSP data (-TT) in panel (3) illustrate that the downgoing wavetrain (the multiples) is comprised mostly of high amplitude surface generated and less prominent interbed multiples. Surface generated multiples are recorded on all of the traces and are manifested as laterally continuous events that arrive after the first break events. Interbed multiples, in contrast, do not extend over the entire depth range. They are present on the deeper traces only (Hinds et al., 1989).

The downgoing waves in panel (3) were separated from the combined wavefield data using an eleven-point median filter and displayed in panel (4). The residual upgoing wave content in panel 4 is minimal. The upgoing waves (panel 5)

were separated by subtracting a scaled version of the downgoing wavefield (panel 4) from the combined wavefield (panel 3) following the methodologies described and Balch and Lee (1984), Hardage (1985), Hinds et al. (1989) and others. The two final panels (6 and 7) in the wavefield separation IPP display the separated upgoing waves (+TT) before and after the application of a three point median filter. The equalized amplitudes of the horizontally aligned Cardium, Viking, Glauconitic, Pekisko, Banff, Wabamun, Nisku, Ireton and Leduc events are interpreted in the final panel and confirmed on the previous panels.

Successful wavefield separation is critical to the interpretation of the VSP data, for any residual upgoing wavefield in panel (4) will be subtracted out of the upgoing wave data. Note that the median filter (panels 4 and 5) has not been particularly effective in separating those upgoing waves that arrive after the first break time on the deepest sonde location trace (panel 4). This, however, is acceptable only because these events are below the zone of interest.

VSP deconvolution

Surface-generated and interbed multiples are totally represented on the separated downgoing wavetrain (Figure 9; panel 4). The initial downgoing pulse (except in the case of head wave contamination) is the primary downgoing P-wave; any downgoing waves that arrive later are a result of multiple reflections. These multiple events can be effectively removed by deconvolving the upgoing wave data with an inverse filter derived from an analysis of the downgoing wavetrain (Hinds et al., 1989). The deconvolution IPP (Figure 10) enables the interpreter to quality control the VSP (up/down) deconvolution process. Panels 1, 2, 6 and 7 in Figures 9 and 10 are bulk time shifted to facilitate the IPP display.

The first two panels (Figure 10) are the non-median and median filtered separated upgoing wavefields. Panels 3 and 4 are the nondeconvolved combined wavefield and separated upgoing data. The fifth panel is the deconvolved upgoing combined wavefield data. Panel 5 represents an example of downgoing wavefield deconvolution applied to the combined (total) wavefield as reported in Smidt (1989). The data following the deconvolution step was then normalized around the first breaks and then corrected for spherical divergence and placed back into -TT time for display. (Note, that the collapsed downgoing wavefield, aligned at 100 ms in panel 5, is muted and absent on the subsequent deconvolved upgoing wavefield panels). A comparison of the nondeconvolved (panel 2) and deconvolved upgoing (panel 7) wavefield data indicates that the deconvolution process has enhanced the frequency content of the upgoing waves and yet preserved the integrity of the primary reflections.

The effect of the multiple interference and the relative success of the deconvolution operator, can be appreciated by the analysis of the Glauconitic event. In panel 2 (Figure 10), the nondeconvolved Glauconitic event is relatively continuous at sonde depths below the Cardium (1825m). At shallower depths, the Glauconitic event is partially masked by an interbed multiple that has as its lower generating surface, the top of the Cardium. On the deconvolved panel 7, the Glauconitic event is relatively continuous at all the sonde depths implying that the interfering multiple event has been attenuated.

Note that the Nisku and Leduc events are relatively low amplitude (in comparison to the Nisku and Leduc events on the seismic line away from the VSP well site) possibly as a result of destructive multiple interference. On the nondeconvolved panels (1 and 2), a strong peak exists just above (overlapping) the Nisku event from the shallowest trace out to the 2140 m trace. The Nisku event is

low amplitude in comparison. After deconvolution, the Nisku event is laterally continuous in amplitude. The anomalous multiple induced peak before the deconvolution can be estimated to be up to 5 ms higher than the overlapped Nisku event.

Inside and outside corridor stacks

Multiple contamination on the VSP upgoing waves can be closely examined using the inside and outside corridor stacks of both the nondeconvolved and deconvolved data. The inside corridor stack of the nondeconvolved data contains both the primary and multiple events, whereas the outside corridor stack data should be relatively free of multiples. If the deconvolution is successful in removing the multiples, then both the inside and outside corridor stacks for the deconvolved data will be predominated by primary reflections.

In Figure 11, the inside and outside corridor stacks of the nondeconvolved data plus the input data to the muting and stacking processes are displayed. The inside and outside corridor stacks differ significantly at the Cardium, Banff, Wabamun, Nisku, and to a lesser extent the Leduc, suggesting that significant multiple interference is observed on the inside corridor stacks. The difference between the displays is attributed to the relative absence of multiples on the outside corridor stack.

A comparison of the inside and outside deconvolved corridor stacks (Figure 12), indicates that multiple interference was substantially attenuated by deconvolution. More specifically, note that the inside and outside corridor stacks of the deconvolved data are similar, suggesting that deconvolution has effectively attenuated the multiple contamination evident on the inside corridor stack of the

nondeconvolved data (panel 1; Figure 11).

Integrated interpretation

On the left-hand side of Figure 13, the post-VSP interpretation of the conventional surface seismic line (Figures 7, 8, 14, and 15) is displayed. A synthetic seismogram for the VSP well, the nondeconvolved inside corridor stack of the VSP data, and the deconvolved outside corridor stack are time-tied to the seismic line at the VSP well site (CDP number 127). The inside and outside corridor stacks and the synthetic seismogram, juxtaposed between the two separated parts of the seismic section at the VSP well location, allows for the evaluation of the synthetic seismogram in indicating the time location of the Leduc.

On the right-hand side of Figure 13, the VSP data are time-tied to the seismic line, the deconvolved outside corridor stack, the VSP well synthetic seismogram, the VSP well velocity log, and the VSP well gamma ray log. The horizontal scale (depth axis) of the VSP display and the scale used for the horizontally-oriented VSP well sonic and gamma ray log depth displays are the same. The outside corridor stack (containing predominantly primary events), the synthetic seismogram, and the two well logs (converted to time) allow for the comparison of the corridor stack, the synthetic seismogram, and the well log data. Because the synthetic seismogram is calculated from the finely depth samples sonic log, in the same area the synthetic will have higher resolution than the corridor stack. Since the range of the wavelengths contained in the VSP are the same as for surface seismic, in most cases the outside corridor stack interpretation will tie to the seismic data interpretation more closely.

The VSP well sonic and gamma logs in Figure 13 are displayed in depth and plotted immediately above the VSP data. The correlation between these data can be illustrated by considering the top of the Wabamun. The top of the Wabamun in the VSP well is represented by the shale/carbonate contact at a depth of 2616 m. The nearest shallower sonde location (depth trace) is at 2610 m; the sonde location immediately below the Wabamun is at 2630 m. The Wabamun event is therefore identified as the trough located in time between the first breaks for the 2610 and 2630 sonde depths (approximately 1450 ms). In a similar fashion, the other seismic events can be identified can be directly correlated to the surface seismic line at CDP number 127, the nondeconvolved inside corridor stack, the deconvolved outside stack, and the synthetic seismogram, velocity and gamma log (in time) for the VSP well.

The event of greatest interest on these data is the Leduc. Note that this reflection, on the VSP data and on the surface seismic near the VSP well site, is one cycle lower than initially interpreted (pre-VSP interpretation shown in Figures 7 and 8). The revised surface seismic interpretation is presented in Figures 14 and 15. The VSP surface seismic correlation clearly indicates that the Leduc top was incorrectly identified at the VSP well site on the pre-VSP interpretation. This miscorrelation explains why the Leduc top came in 80 m low relative to prognosis, it does not however explain why the surface seismic line was originally misinterpreted. The reason these data were initially misinterpreted is that the interval on the seismic line between CDP numbers 100 and 140 is anomalous (Figures 14 and 15).

On the reinterpreted seismic profile (Figures 14 and 15), the trace interval 100 to 140 is characterized by:

- 1) Positive time-structural relief (on the order of 5 ms) along both pre-Leduc and deeper post-Leduc events;
- 2) An anomalously low-amplitude Leduc event; and
- 3) An anomalous reflection pattern within the Wabamun/Leduc interval.

As previously indicated, these anomalous seismic signatures were initially interpreted as reef diagnostic and were attributed to an envisioned 80 m of anomalous accretionary reef growth. The time-structural relief along pre- and post-Leduc events in particular were attributed to velocity pullup and drape, respectively.

The VSP well conclusively established that the Leduc was missidentified on the original interpretation (Figures 7 and 8) and that the observed seismic anomalies are not related to an anomalous, late stage accretionary reef growth. What then is the origin of these anomalies? There appear to be four principal and potentially superposed sources:

- 1) Anomalous structural relief at the top of the pre-Cretaceous subcrop between traces 100 and 140;
- 2) Stratigraphic anomalies within the Winterburn Group (Figure 1); and
- 3) Multiple interference within the Wabamun/Leduc interval.
- 4) tuning effects associated with the thinning of the Ireton between traces 100 and 140.

It is possible that the observed time-structural anomalies (positive relief on the order of 5 ms) between traces 100 and 140 are caused by erosional relief at the pre-Cretaceous subcrop. As illustrated by the velocity log (Figure 13), the upper Mississippian has a higher velocity than the overlying Cretaceous sediment. Positive erosional relief at the pre-Cretaceous subcrop would cause underlying events to be time structurally "pulled-up"; the overlying events would be draped as a result of compaction (Anderson et al., 1989). Such erosional relief at the pre-Cretaceous horizon could also cause lateral variations in the multiple interference pattern and thereby contribute to the character anomaly observed within the Wabamun/Leduc interval between traces 100 and 140.

An alternative explanation for the observed time-structure and amplitude anomalies is a lithologic variation within the Winterburn Group. It is possible that a localized Nisku Formation (Winterburn Group) patch reef (Rennie et al., 1989) has developed above the underlying Leduc reef between traces 100 and 140. Such a carbonate buildup would be characterized on seismic data by velocity pullup, time-structural drape, and lateral character variations within the Winterburn Group. Unfortunately, due to the absence of core control within the Winterburn Group, this thesis cannot be confirmed; however we can confirm that the Nisku Formation in the VSP well is productive and 8 m thicker than at well 6-6. This additional Nisku buildup and its associated porosity could contribute to the observed time-structural and character anomalies.

Another possibility is that character anomaly observed between traces 100 and 140 are partially tuning effects, caused by the subtle thinning of Ireton (as highlighted on the north-south geologic cross-section of Figure 6). Such thinning of the Ireton is also illustrated on the isopach contour map of Figure 16. This Figure

shows that the north-south oriented seismic line traverses thinner Ireton between traces 100 and 140 than elsewhere.

As indicated in the preceding discussions, the character and time-structural anomaly observed between traces 100 and 140 can be explained as the superposed effects of one or more geologic causes. Given the absence of additional subsurface control this is the extent to which the source of the anomaly can be pinpointed. All that can be stated with absolute certainty is that the anomaly is not due to thick (on the order of 80 m), late-stage accretionary reef growth as originally thought.

Summary

The VSP well was drilled into the Leduc reef at Lanaway Field, south central Alberta, in order to evaluate an anomaly observed on surface seismic data. The pre-VSP well interpretation of these seismic data suggested that the VSP well would encounter up to 80 m of anomalous accretionary reef growth at the Leduc level. However, drilling confirmed that the Leduc at the VSP well site was more-or-less regional. In order to elucidate the discrepancy between the pre-well seismic interpretation and the drilling results, a near-offset VSP was run at the VSP well site.

The interpretively processed VSP data provided valuable information regarding the origin of the seismic anomaly observed in the vicinity of the VSP well site. On the basis of these data the operator was able to:

- 1) Establish that the Leduc event had been miscorrelated on the pre-well seismic interpretation;

- 2) Correctly correlate the Leduc event at the VSP well site;
- 3) Determine that the seismic anomaly at the VSP well site was not a processing artifact; and
- 3) Further elucidate the geologic origin of the seismic anomaly.

On the basis of VSP data, the operator was able to establish that the observed seismic anomaly at the VSP well was most likely attributable to one or more superposed effects:

- 1) Velocity-pullup and structural drape due to anomalous erosional relief at the pre-Cretaceous subcrop, and the effects of associated interbed multiple reflections;
- 2) Localized patch reef development within the Winterburn Group; and
- 3) Tuning due to thinning of the Ireton Formation in the vicinity of the VSP well.

Due the absence of additional subsurface seismic and well control, the exact cause of the observed anomaly cannot be determined. All that can be stated with absolute certainty is that the anomaly is neither a processing artifact nor due to the presence of a thick late-stage accretionary reef growth as originally interpreted.

References

AGAT Laboratories, 1988, Table of formations of Alberta: AGAT Laboratories, Calgary.

Anderson, N.L., Brown, R.J., and Hinds, R.C., 1989a, Low- and high-relief Leduc Formation reefs: A seismic analysis: *Geophysics*, 54, 1410-1419.

Anderson, N.L., White, D., and Hinds, R.C., 1989, Woodbend Group reservoirs, *in*, Anderson, N.L., Hills, L.V., and Cederwall, D.A., Eds, Geophysical atlas of western Canadian hydrocarbon pools: *Can. Soc. Expl. Geophys./Can. Soc. Petr. Geol.*, 101-132.

Balch, A.H., and Lee, M.W., (eds), 1984, Vertical seismic profiling- techniques, applications and case histories: *Int. Human Res. Devel. Corp.*, Boston, 488 p.

Beydoun, W.B., 1985, Asymptotic wave methods in heterogeneous media: unpublished Ph.D. thesis, Massachusetts Institute of Technology.

Dillon, P.B., and Thomson, R.C., 1984, Offset source VSP surveys and their image reconstruction: *Geophys. Prosp.* 32, 790-811.

Hardage, B.A., 1985, Vertical seismic profiling: *Geophys. Press*, London, 2nd edition, 509 p.

Hinds, R.C., Kuzmiski, R.K., Botha, W.J., and Anderson, N.L., 1989, Vertical and lateral seismic profiles, *in*, Anderson, N.L., Hills, L.V., and Cederwall, D.A., Eds, Geophysical atlas of western Canadian hydrocarbon pools: *Can. Soc. Expl. Geophys./Can. Soc. Petr. Geol.*, 319-344.

Hinds, R.C., 1991, Seismic signatures and integrated exploration: Newsletter of the South African Geophys. Assoc., July issue, 10-12.

Klovan, J.E., 1964, Facies analysis of the Redwater reef complex, Alberta, Canada: Bull. Can. Petr. Geol., 12, 2260-2281.

Moore, P.F., 1988, Devonian geohistory of the western interior of Canada, *in*, McMillan, N.J., Embry, A.F., and Glass, D.J., Eds., Devonian of the World: Can. Soc. Petr. Geol. Memoir 14, 67-87.

Moore, P.F., 1989a, Devonian reefs in Canada and some adjacent areas, *in*, Geldsetzer, H.H.J., James, N.P., and Tebbutt, G.E., Eds., Reefs, Canada and Adjacent areas: Can. Soc. Petr. Geol. Memoir 13, 367-390.

Moore, P.F., 1989b, The Kaskaskia Sequence: reefs, platforms and foredeeps, The lower Kaskaskia Sequence - Devonian, *in*, Ricketts, B.D., Eds., Western Canada sedimentary basin, a case history: Can. Petr. Geol., 139-164.

Mossop, G.D., 1972, Origin of the peripheral rim, Redwater reef, Alberta: Bull. Can. Petr. Geol., 20, 238-280.

Mountjoy, E., 1980, Some questions about the development of Upper Devonian carbonate buildups (reefs), Western Canada: Bull. Can. Petr. Geol., 28, 315-344.

Rennie, W., Leyland, W., and Skuce, A., 1989, Winterburn (Nisku) reservoirs, *in*, Anderson, N.L., Hills, L.V., and Cederwall, D.A., Eds, Geophysical atlas of western Canadian hydrocarbon pools: Can. Soc. Expl. Geophys./Can. Soc. Petr. Geol., 133-

154.

Smidt, J.M., 1989, VSP processing with full downgoing-wavefield deconvolution applied to the total wavefield, *First Break*, 7, no. 6, 247-257.

Stoakes, F.A., 1980, Nature and control of shale basin fill and its effect on reef growth and termination: Upper Devonian Duvernay and Ireton Formations of Alberta, Canada: *Bull. Can. Petr. Geol.*, 28, 345-410.

Stoakes, F.A., and Wendte, J.C., 1987, The Woodbend Group, *in*, Krause, F.F., and Burrows, O.G., Eds., *Devonian lithofacies and reservoir styles in Alberta: Second International Symposium Devonian System*, Calgary, 153-170.

Figure Captions

Figure 1. Stratigraphy of the Central Plains area of Western Canada Sedimentary Basin (after AGAT Laboratories, 1988)

Figure 2. Regional location map of the Lanaway study area (with permission of Talisman Resources Inc.)

Figure 3. Detailed map of Lanaway study area showing geological cross-section locations and seismic traverse.

Figure 4. West-east geologic cross-section A-A' (refer to Figure 3 for location). The Leduc in 11-1 is structurally low and wet; 16-1 and 11-6 are productive (Leduc reservoirs); 16-6 and 10-29 are offreef and abandoned.

Figure 5. West-east geologic cross-section B-A' (refer to Figure 3 for location). The Leduc in 11-36 and 2-36 (producing oil from the Nisku) is structurally low and wet; the VSP well is productive (Leduc reservoir); 10-29 is offreef and abandoned. The VSP well has a different oil/water contact than 11-6 to the North (Figure 3) and is assigned to a separate pool.

Figure 6. North-south geologic cross-section C-C' (refer to Figure 3 for location). The Leduc in 11-6 and the VSP well is productive; 6-6 is wet and classified as an abandoned oil well. The cross-section shows the structural relief in the North-south direction between the two producing wells along with associated drape (thickening of the Ireton at 6-6).

Figure 7. North-south oriented example seismic line showing the geophysical interpretation of the VSP well site prior to drilling. Drilling and VSP data confirmed that this pre-well correlation was inaccurate and that the interpreted time-structural anomaly at the Leduc level (traces 100-140) is not attributable to corresponding structural relief. The location of this north-south seismic line is shown in Figure 3.

Figure 8. Enlarged version of the apparent time-structural anomaly at the Leduc level (VSP well site; Figure 6).

Figure 9. Interpretive processing panel depicting the wavefield separation of the near-offset VSP. (1: field data (FRT); 2: balanced field data (FRT); 3: gained field data (-TT); 4: separated downgoing waves (-TT); 5: separated upgoing waves (-TT); 6: upgoing waves (+TT); 7: median filtered upgoing waves (+TT)).

Figure 10. Interpretive processing panel depicting the deconvolution of the near-offset VSP. (1: upgoing waves (+TT); 2: median filtered upgoing waves (+TT); 3: separated downgoing waves (-TT); 4: separated upgoing waves (-TT); 5: deconvolved, upgoing waves (-TT); 6: deconvolved, upgoing waves (+TT); 7: median filtered, deconvolved, upgoing waves (+TT))

Figure 11. Interpretive processing panel illustrating the utility of the nondeconvolved inside and outside corridor stacks. (1: median filtered upgoing waves (+TT); 2: muted outside corridor data (+TT); 3: outside corridor stack; 4: inside corridor stack; 5: muted inside corridor data (+TT); 6: median filtered upgoing waves (+TT))

p5/7Figure 12. Interpretive processing panel illustrating the utility of the deconvolved inside and outside corridor stacks. (1: median filtered, deconvolved upgoing waves (+TT); 2: muted outside corridor deconvolved data (+TT); 3: outside corridor deconvolved stack; 4: inside corridor deconvolved stack; 5: muted inside corridor deconvolved data (+TT); 6: median filtered, deconvolved upgoing waves (+TT))

Figure 13. Integrated interpretive display (IID) showing the interpretation of the available exploration data. The synthetic seismogram was generated using a zero-phase, 30 Hz center frequency Ricker wavelet.

Figure 14. Post-VSP interpretation of the north-south oriented seismic line (location shown in Figure 3). The Leduc event on this display is only slightly time-structurally elevated at the VSP well site. This interpretation is consistent with well log control.

Figure 15. Enlarged version of the post-VSP interpretation of the north-south oriented seismic line (location shown in Figure 3).

Figure 16. Ireton isopach map showing the drape of the Ireton along the example seismic line (Figure 14 and 15). Considerable time-structural relief along the Ireton event can be correlated from the seismic to the isopach map (as highlighted by arrows in Figure 14).

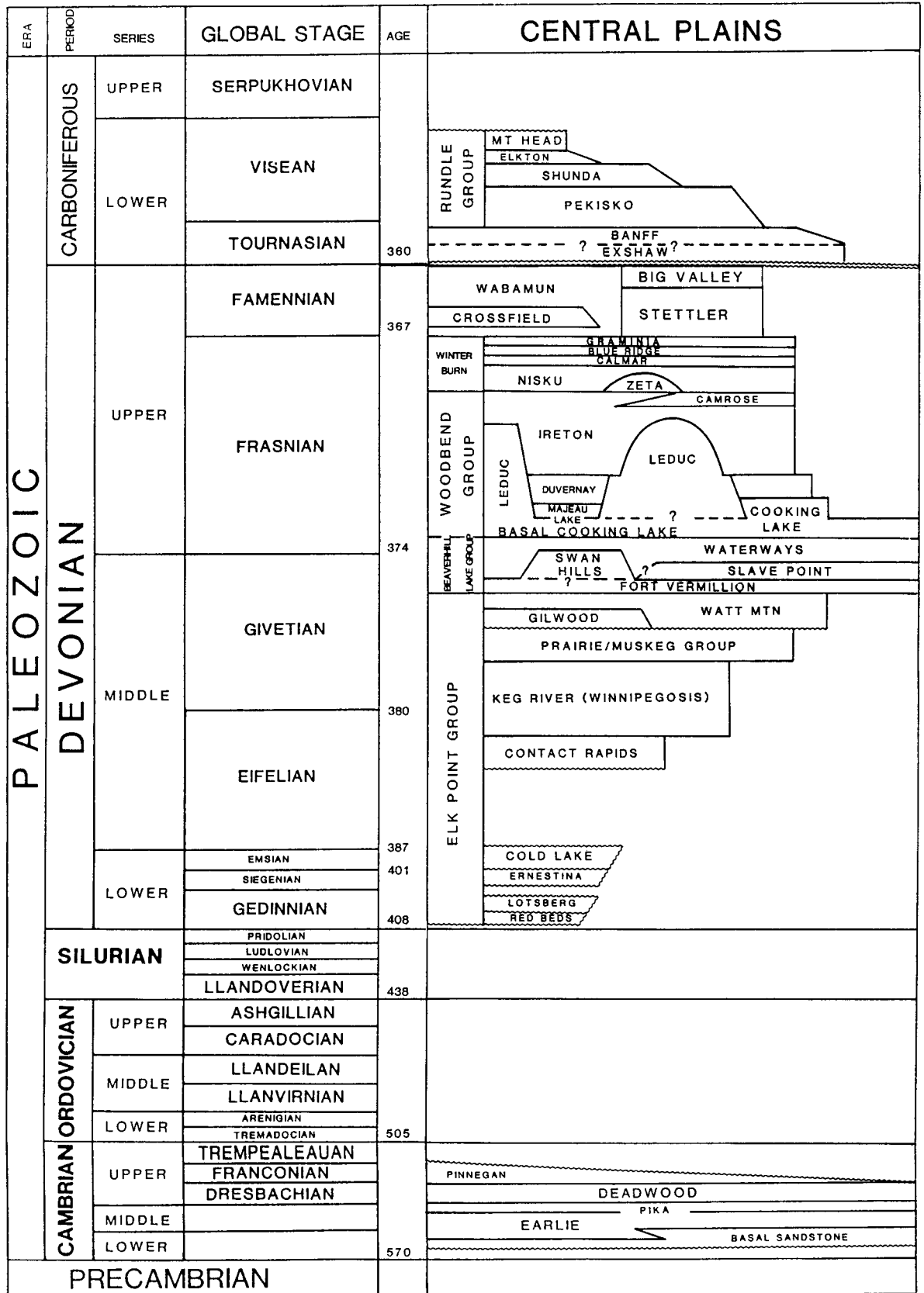


Figure 1.

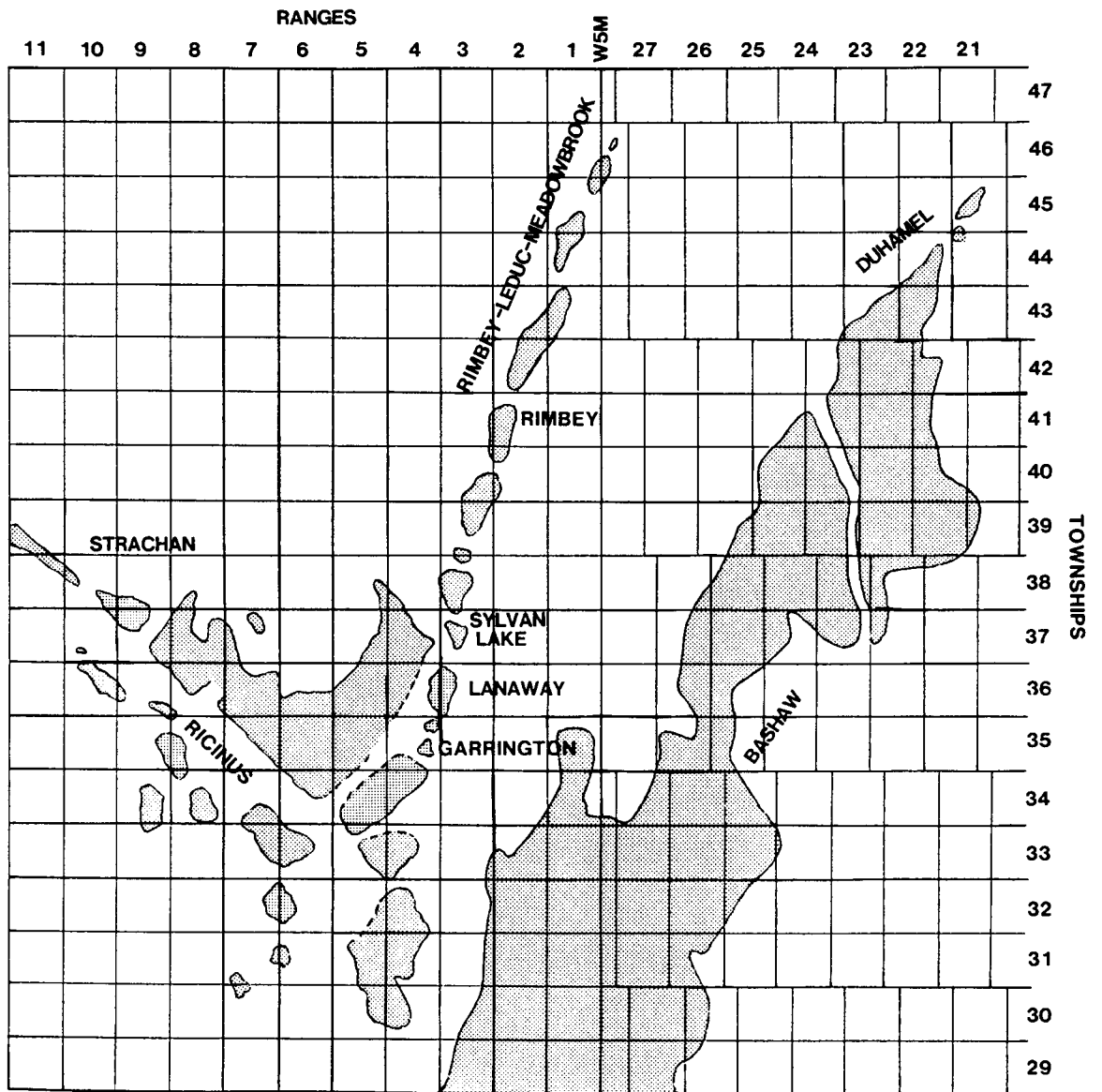
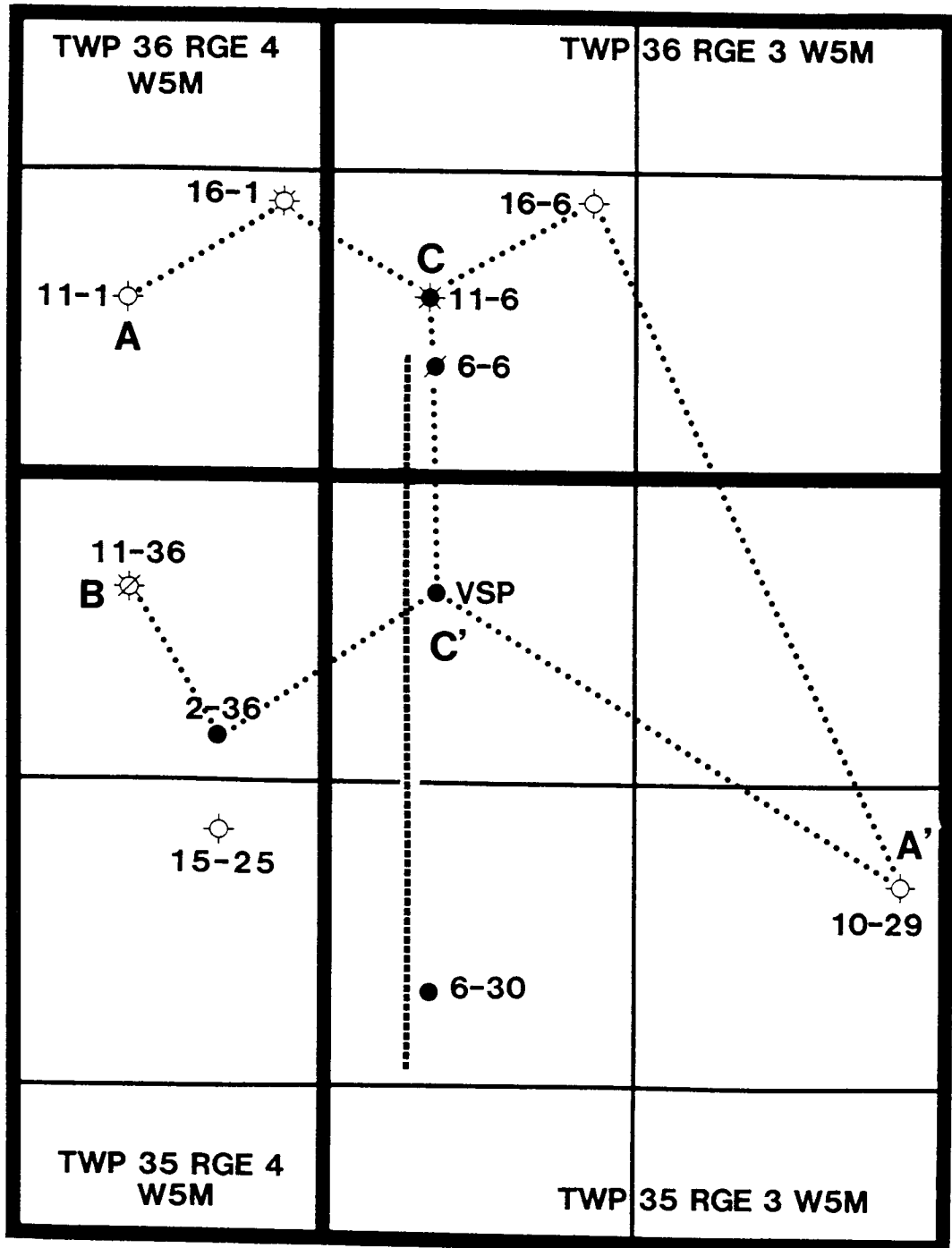


Figure 2.

1 MILE

SCALE



GEOLOGIC CROSS-SECTION

SEISMIC SECTION

Figure 3.

Figure 4.

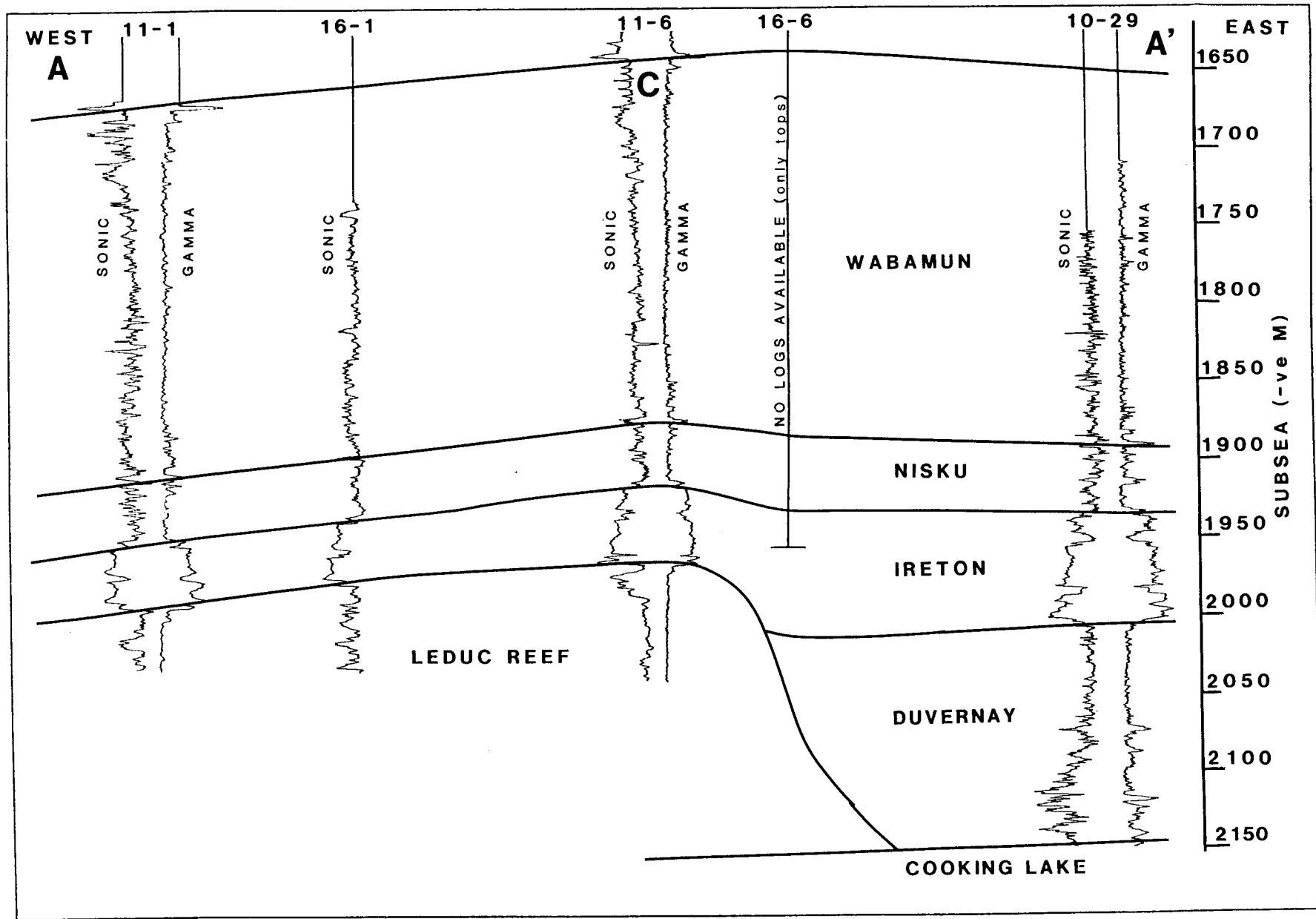


Figure 5.

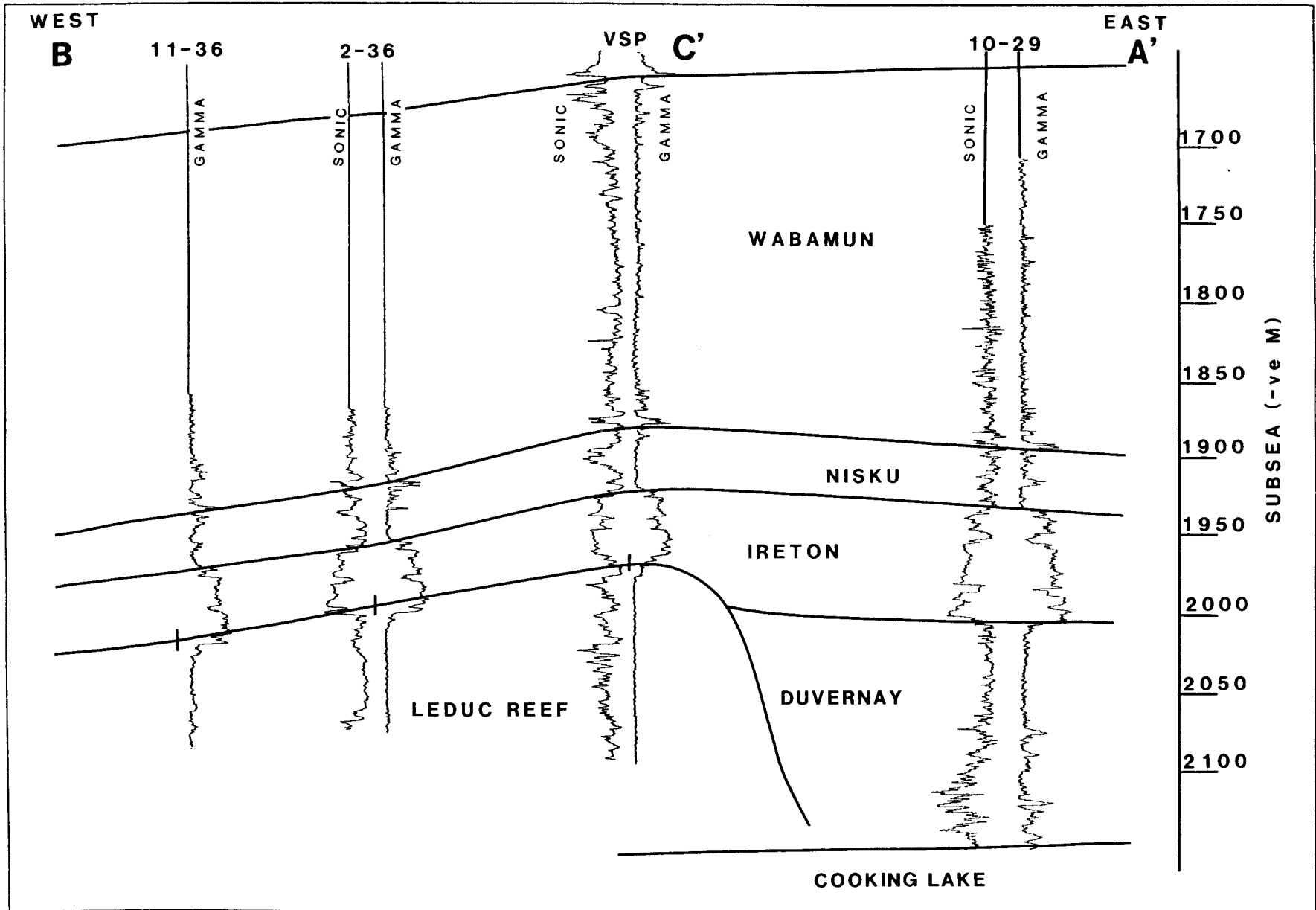
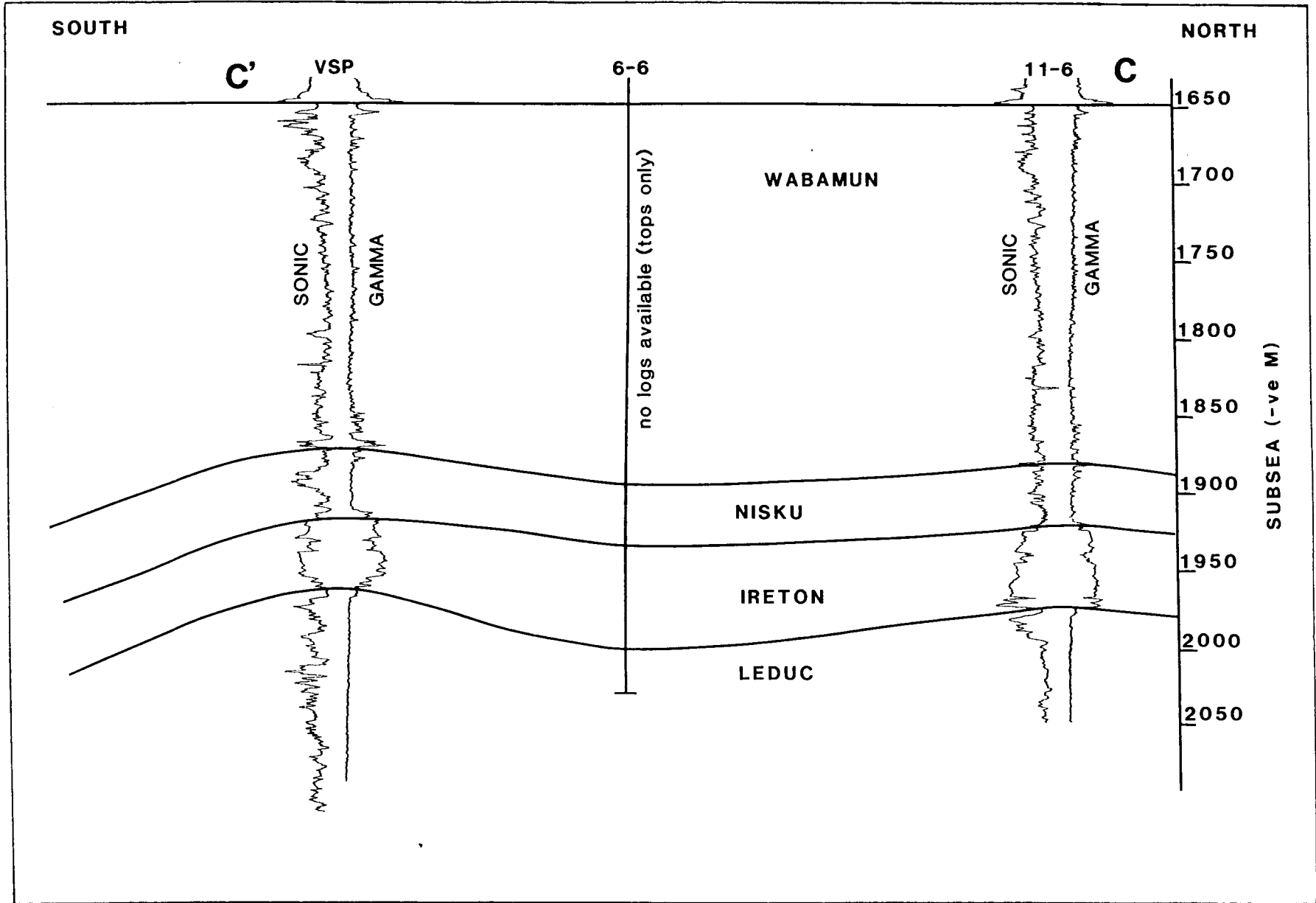


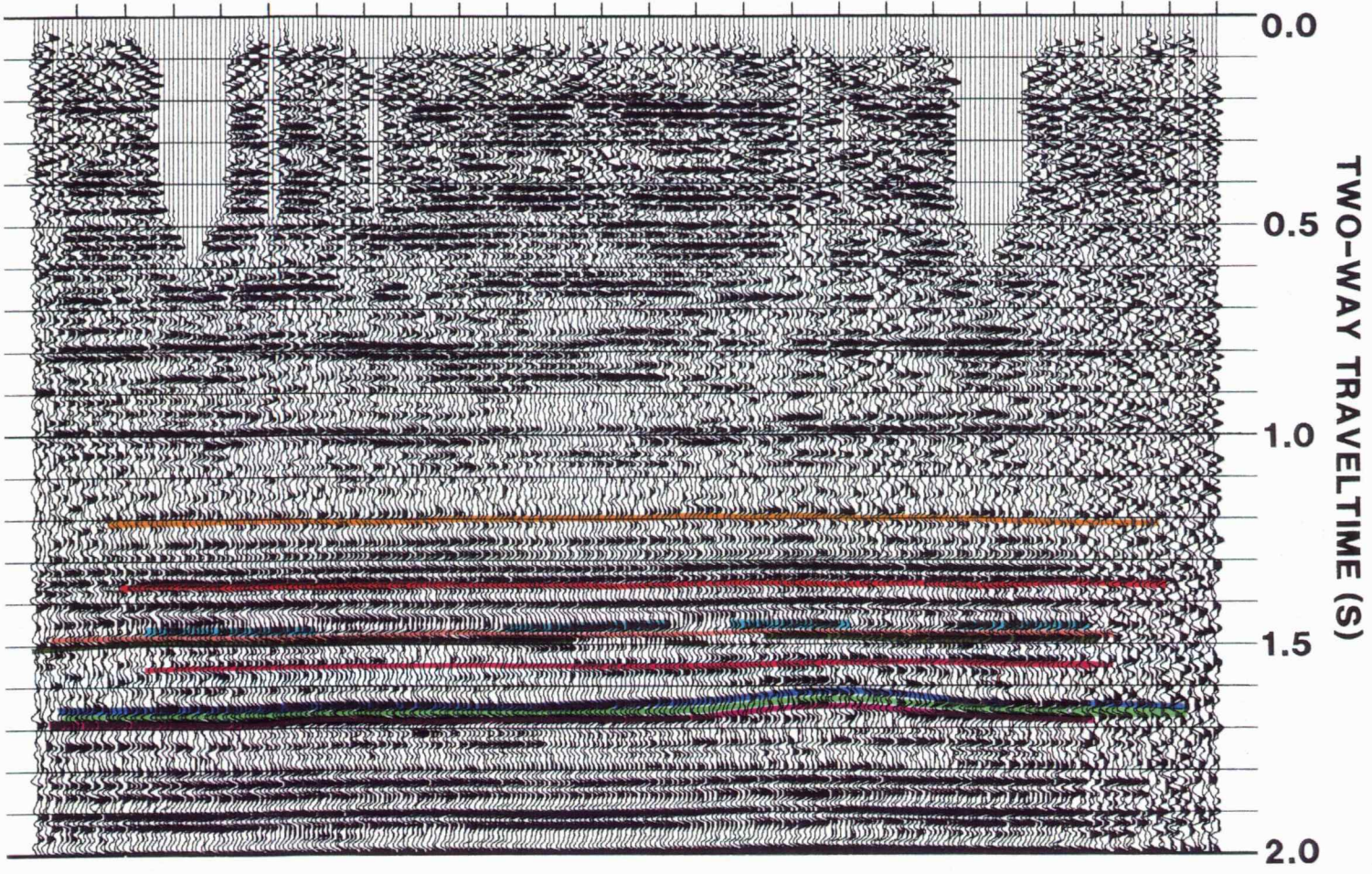
Figure 6.



SOUTH

NORTH

281 271 261 251 241 231 221 211 201 191 181 171 161 151 141 131 121 111 101 91 81 71 61 51 41 CDP



- CARDIUM
- VIKING
- GLAUCONITIC
- PEKISKO
- BANFF
- WABAMUN
- NISKU
- IRETON
- LEDUC

SCALE

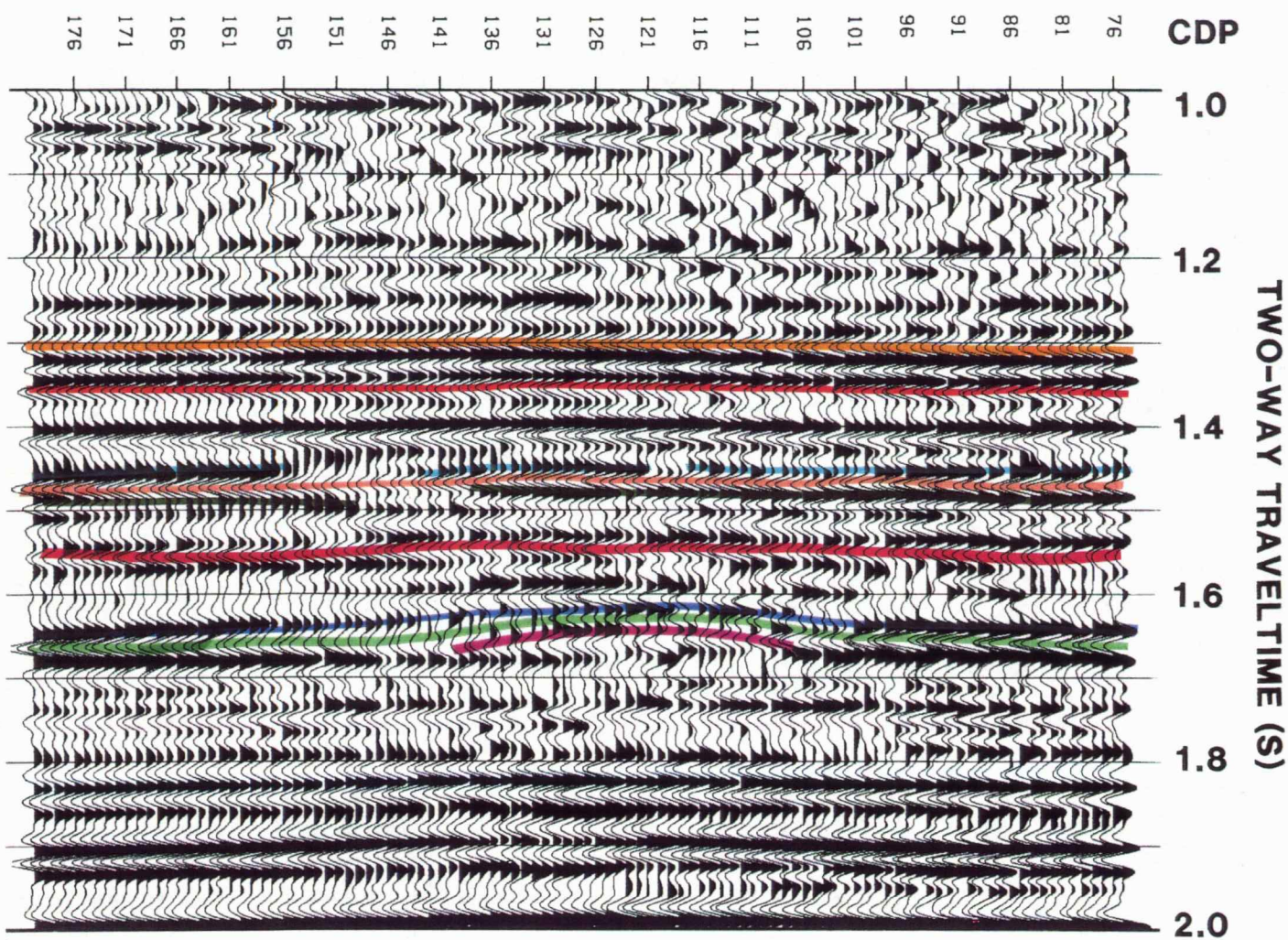


1 KM

Figure 7.

SOUTH

NORTH



CARDIUM



VIKING



GLAUCONITIC



PEKISKO



BANFF



WABAMUN



NISKU



IRETON



LEDUC



Figure 8.

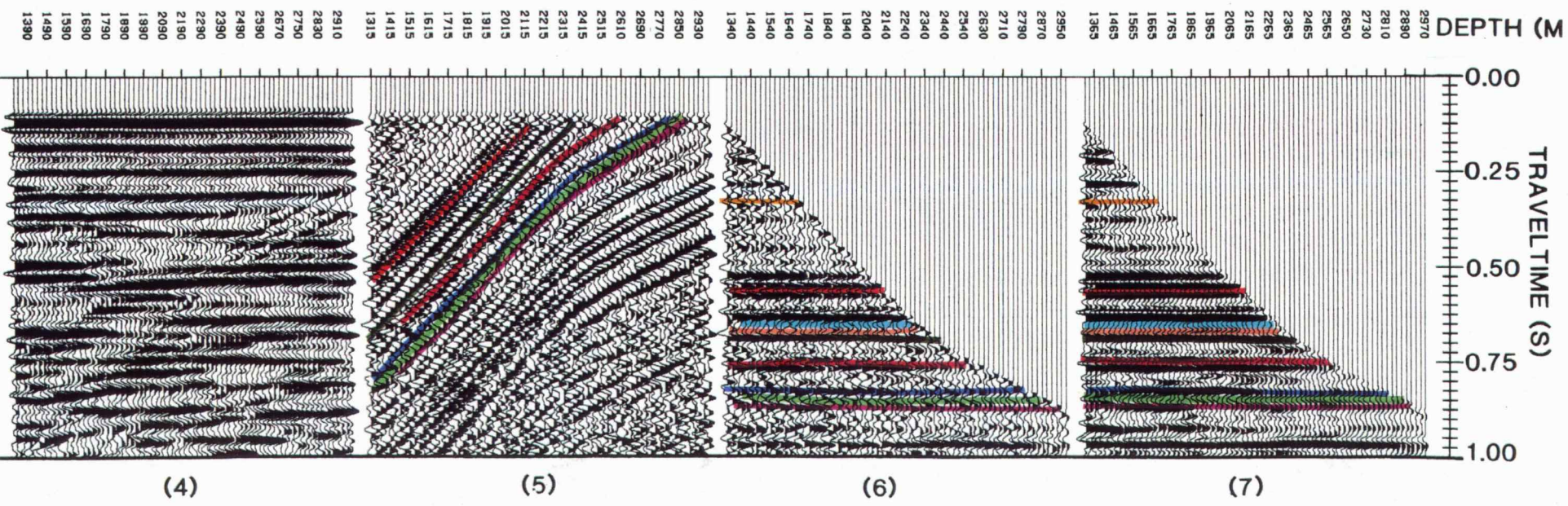
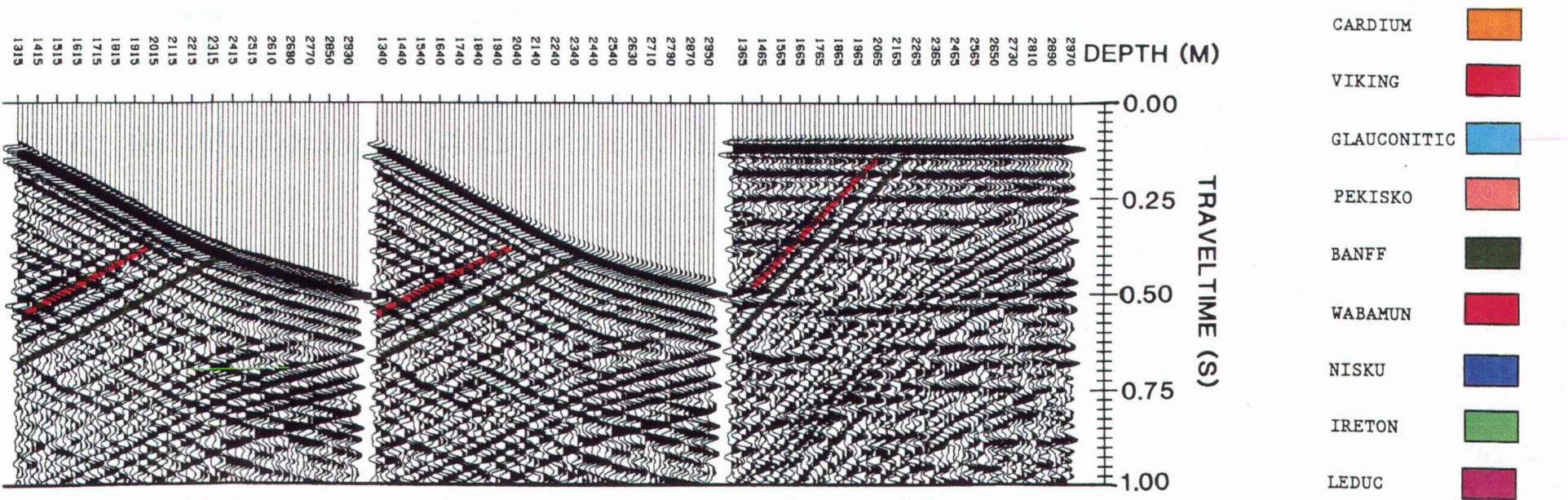


Figure 9.

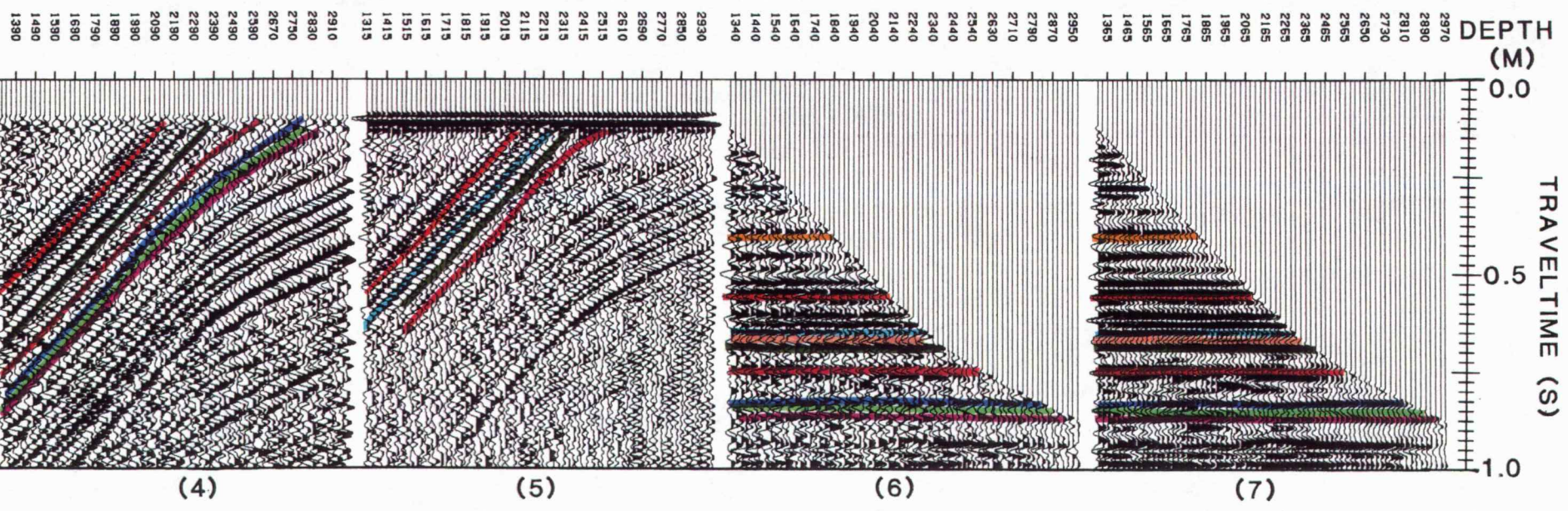
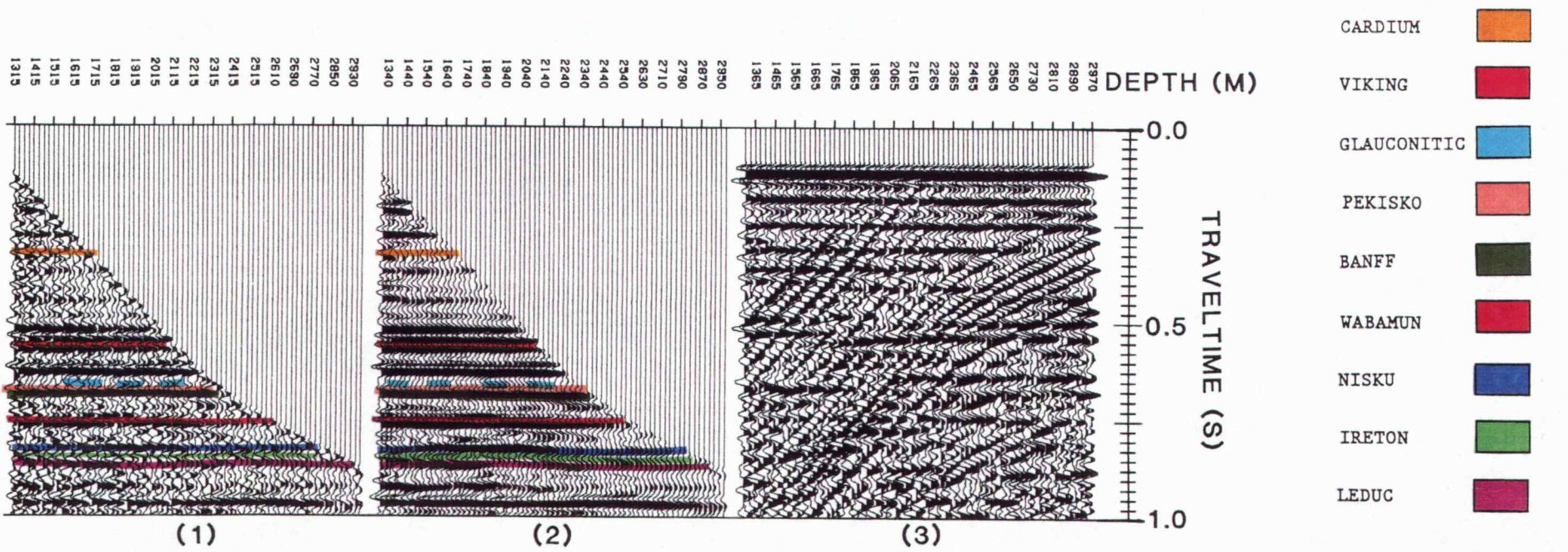


Figure 10.

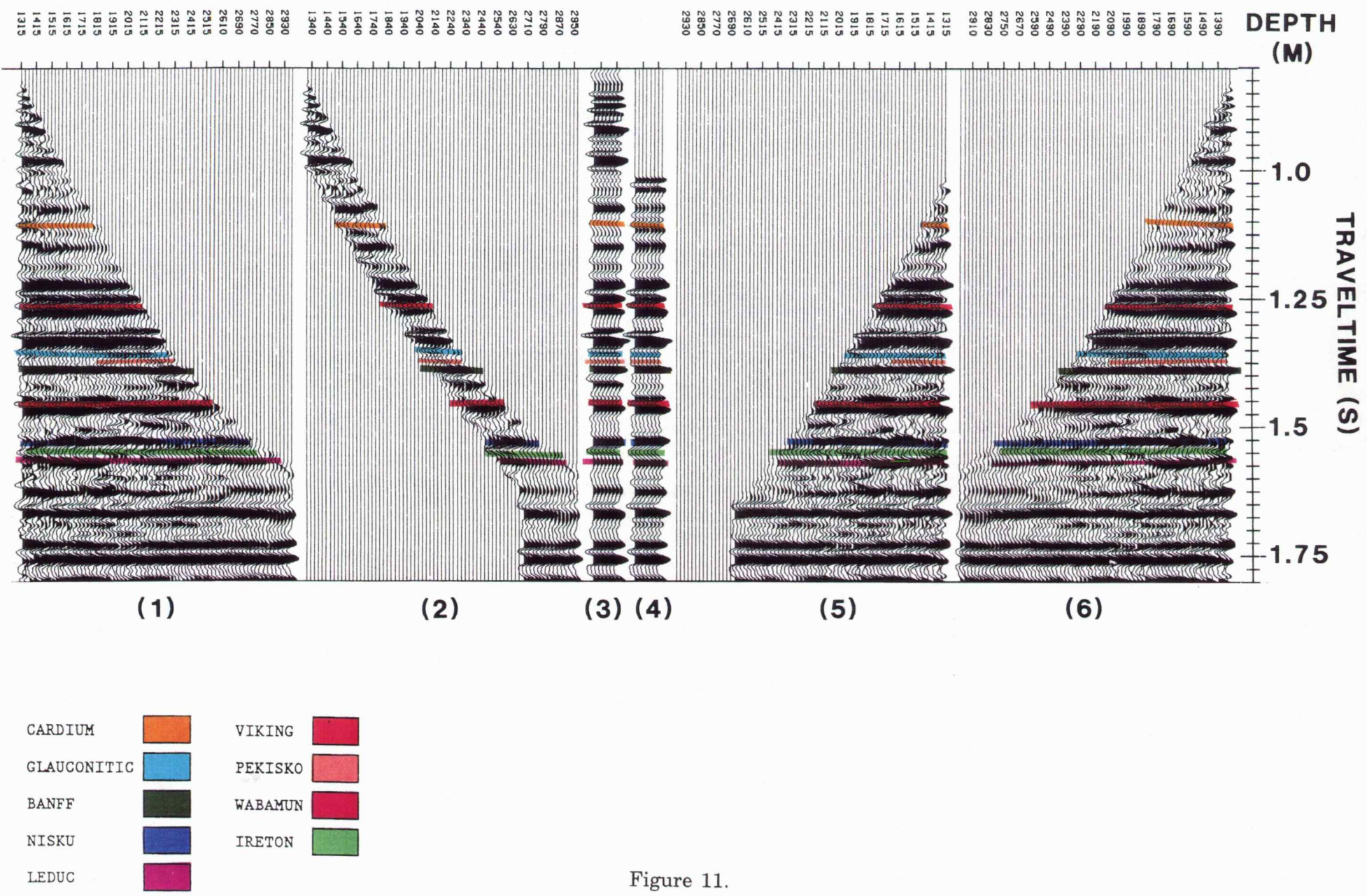
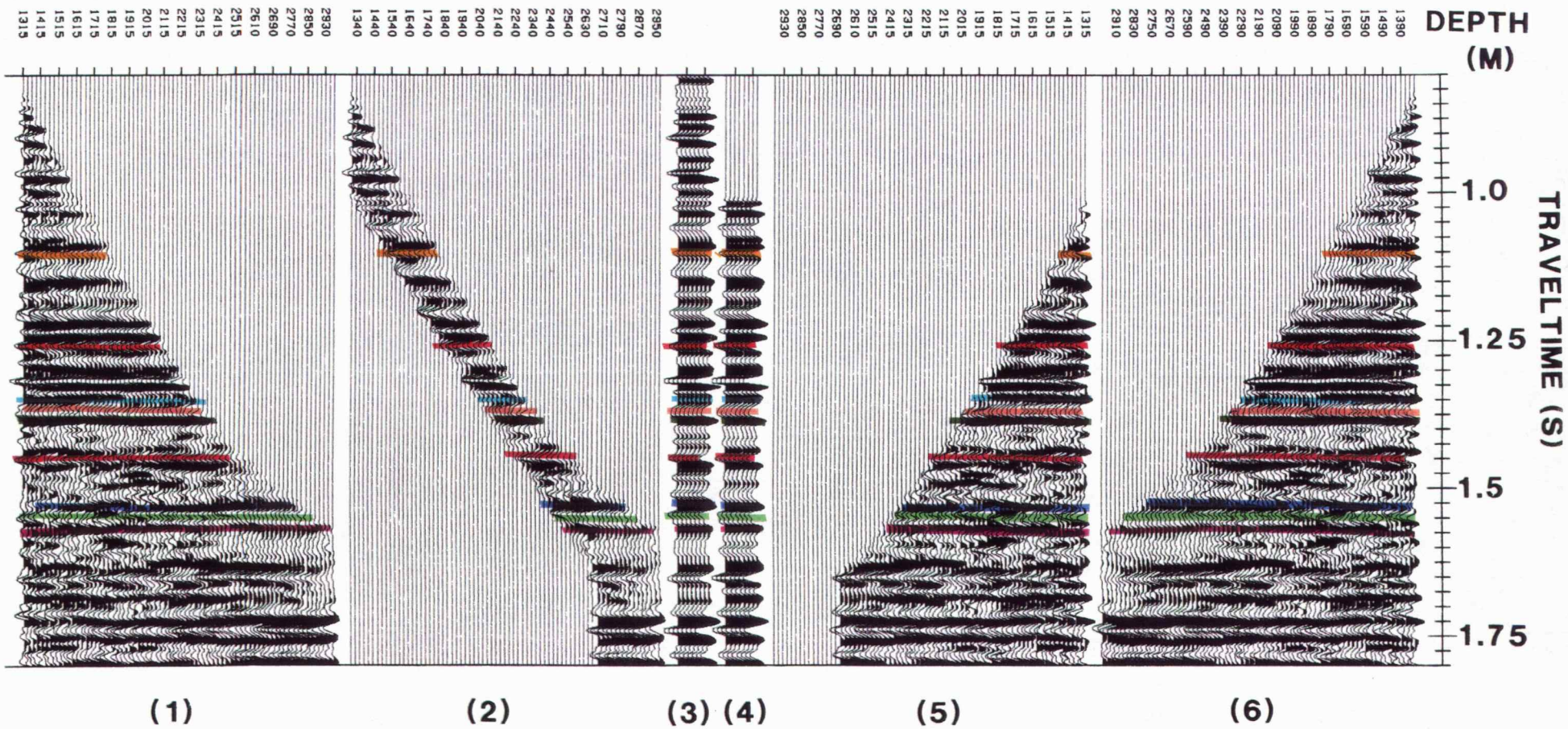


Figure 11.



CARDIUM		VIKING	
GLAUCONITIC		PEKISKO	
BANFF		WABAMUN	
NISKU		IRETON	
LEDUC			

Figure 12.

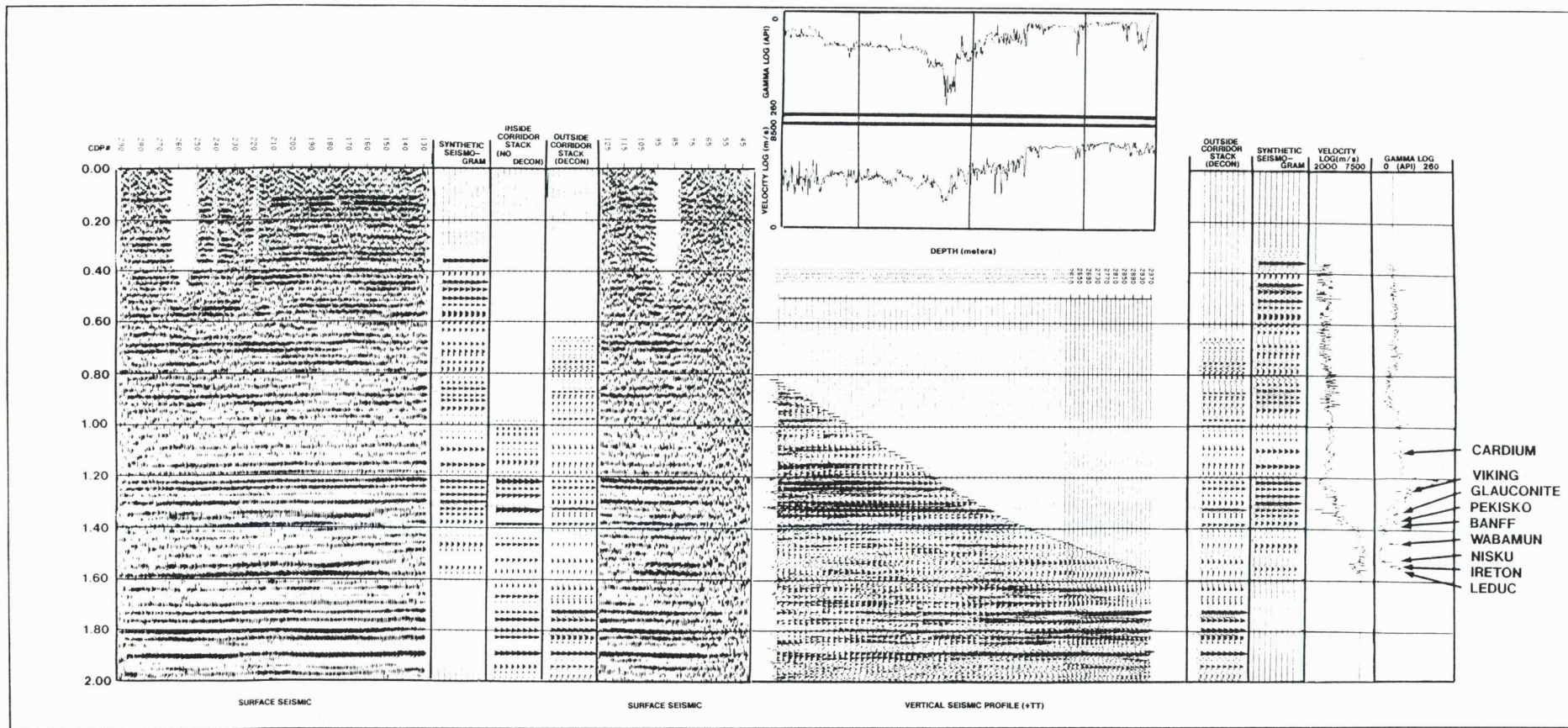
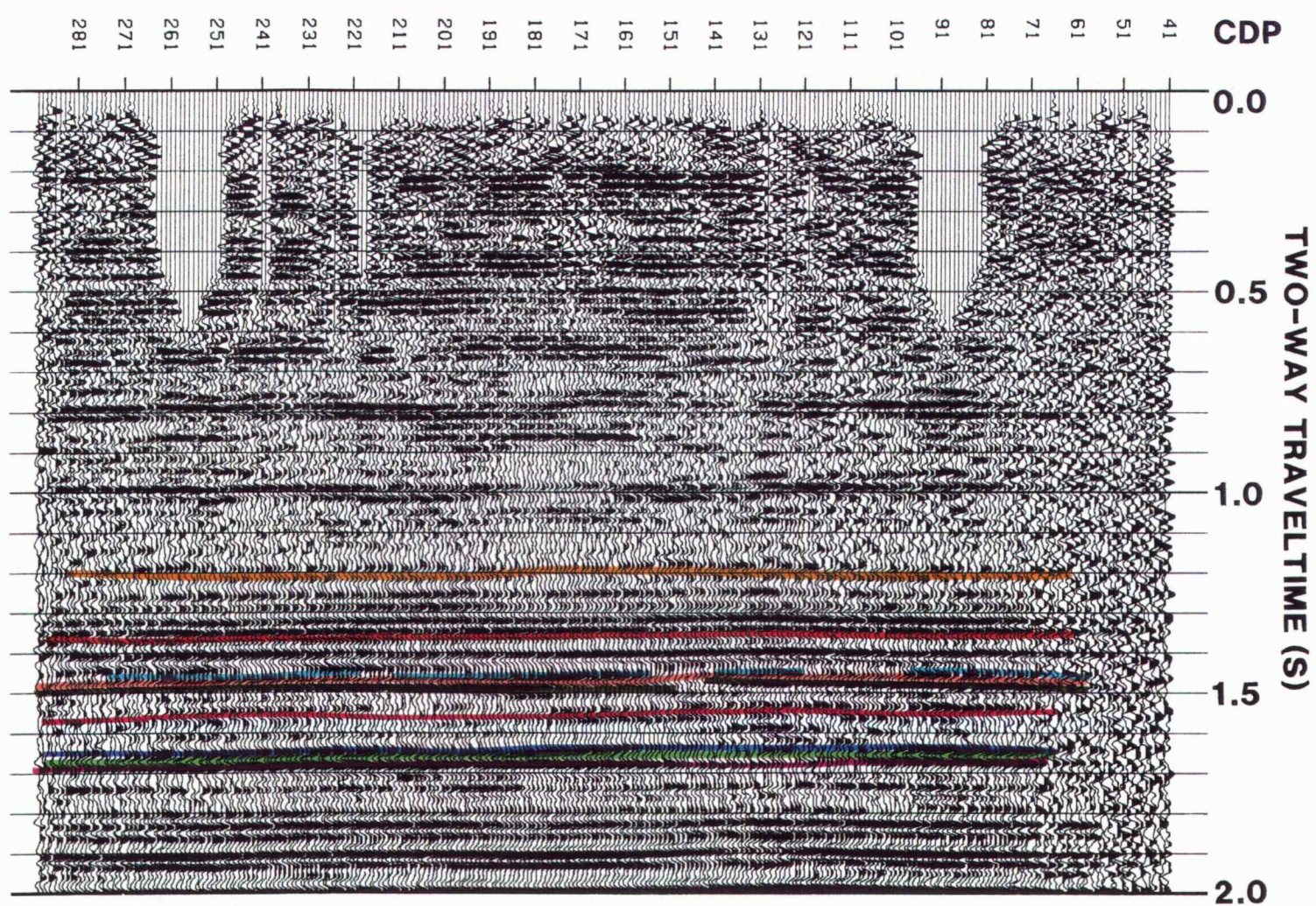


Figure 13.

SOUTH

NORTH



CARDIUM

VIKING

GLAUCONITIC

PEKISKO

BANFF

WABAMUN

NISKU

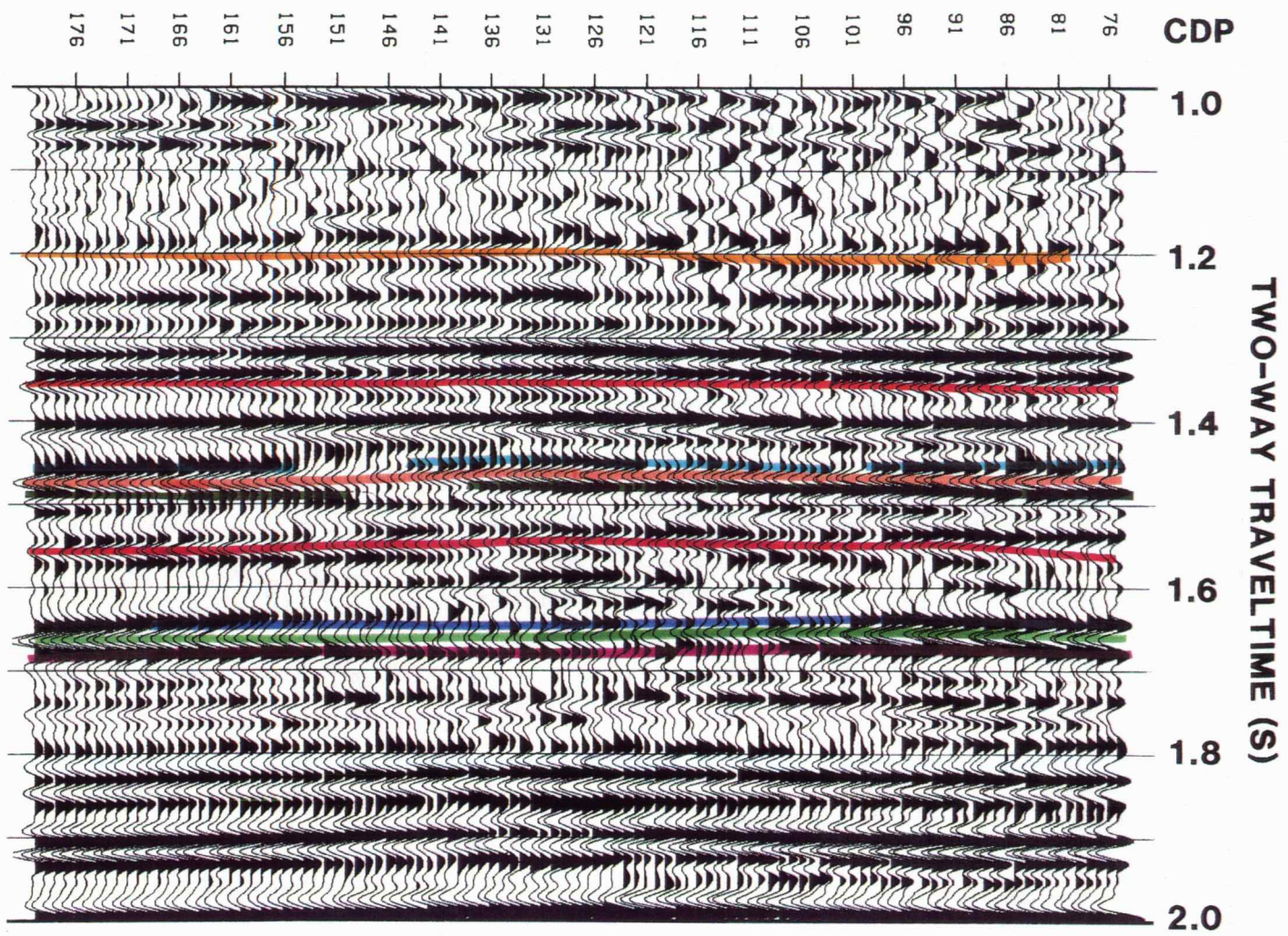
IRETON

LEDUC

Figure 14.

SOUTH

NORTH



CARDIUM

VIKING

GLAUCONITIC

PEKISKO

BANFF

WABAMUN

NISKU

IRETON

LEDUC



Figure 15.

SCALE 1 MILE

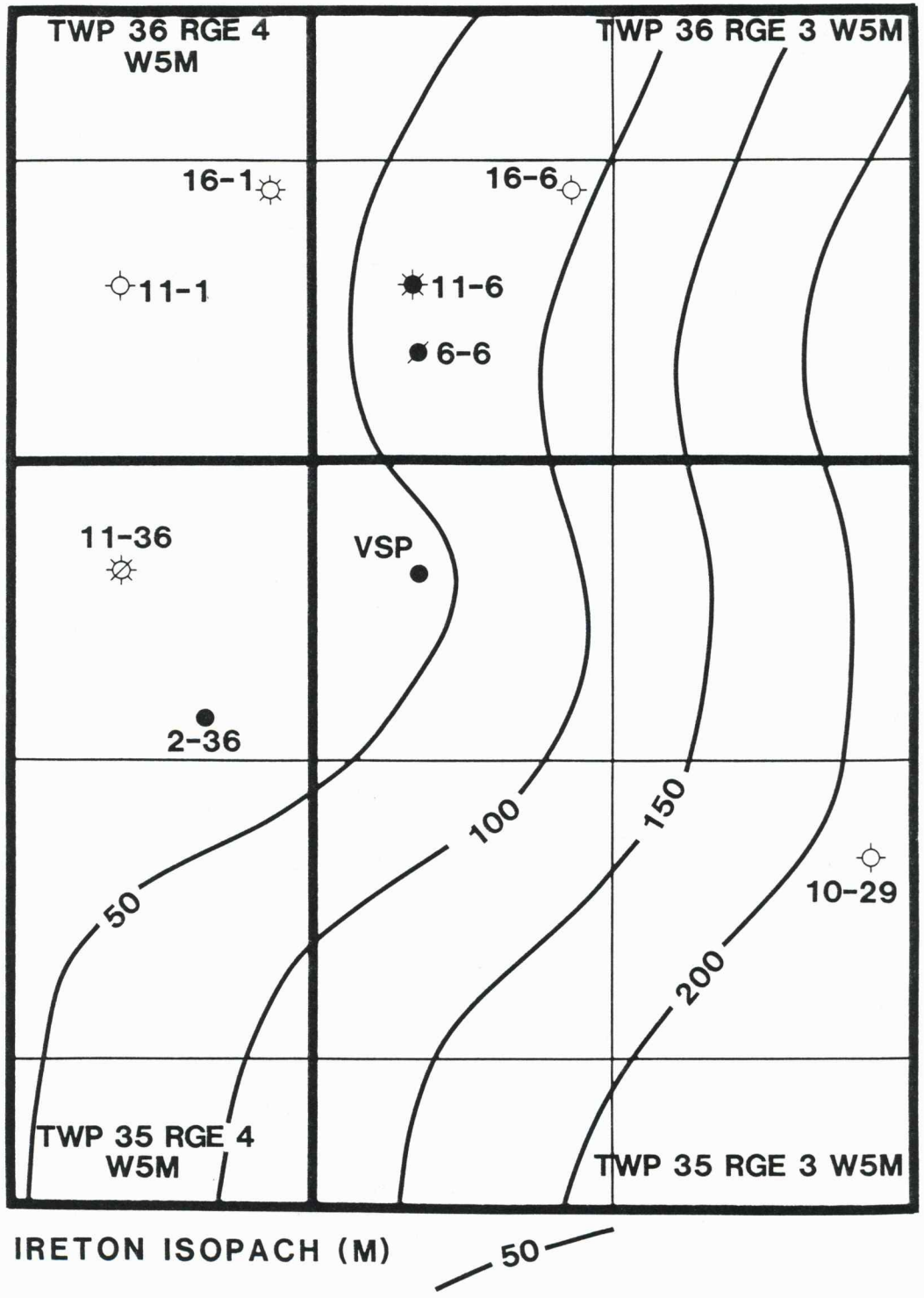


Figure 16.